Application of the grid convergence index to a laminar axisymmetric sudden expansion flow

Verónica M. Carrillo[1,2], John E. Petrie[1], Esteban A. Pacheco[2]

[1] Albrook Hydraulics Laboratory, Department of Civil and Environmental Engineering, Washington State University, 405 Spokane Street, Pullman WA, USA, 99164-2910.

[2] Department of Civil Engineering, Hydraulics & Fluid Dynamics Laboratory, Universidad de Cuenca, Av. 12 de Abril y Agustin Cueva, Cuenca, Ecuador, 010150.

Autores para correspondencia: v.carrilloserrano@email.wsu.edu, j.petrie@wsu.edu, esteban.pacheco@ucuenca.edu.ec

Fecha de recepción: 21 de septiembre de 2014 - Fecha de aceptación: 20 de octubre de 2014

RESUMEN

El uso de modelos numéricos para la representación de procesos naturales es cada vez más común, gracias al desarrollo de herramientas avanzadas problemas cada vez más complejos pueden ser abordados. Sin embargo, mientras sistemas avanzados pueden ser solventados, la incertidumbre de la precisión de la solución obtenida se mantiene. La comparación entre los valores experimentales y los obtenidos mediante las simulaciones no es evidencia suficiente de la calidad de los resultados. El método del índice de convergencia de la grilla (GCI) se propone como una alternativa para calcular y reportar la estimación del error de discretización en la aplicación de mecánica de fluidos computacional (CFD) para las simulaciones, este método permite la estimación del error de discretización mediante la aplicación de la teoría de Extrapolación de Richardson, este procedimiento es aplicado a un caso de flujo laminar en una tubería que experimenta una expansión repentina. Los resultados de un estudio experimental se utilizan para verificar tanto la simulación numérica como los resultados de GCI. Como resultado de la aplicación de este método el orden de precisión del esquema numérico utilizado fue verificado. Comparando los resultados numéricos con los valores experimentales se obtuvo un máximo error de 6%. Finalmente, considerando las dos grillas más finas se puede concluir que el rango asintótico se ha alcanzado y que una grilla más fina no mejorara considerablemente la precisión de la solución como lo hará el costo del procedimiento.

Palabras clave: Análisis de incertidumbre, dinámica de fluidos computacional, extrapolación de Richardson, error de discretización.

ABSTRACT

The use of numerical models to represent natural processes is increasingly common. The development of advanced numerical tools allows a more physically-based representation of complex flow phenomena. While more advanced systems can be solved, the uncertainty of the accuracy of the solutions obtained remains. The mere comparison between experiments and simulations is not enough proof of strength of the results. The Grid Convergence Index (GCI) methodology has been proposed with the aim to provide a mechanism to calculate and report discretization errors estimates in computational fluid dynamics (CFD) simulations. It permits the quantification of the uncertainty present in grid convergence. This method uses a grid convergence error estimator that is obtained by applying the generalized Richardson Extrapolation theory. The process is applied to an axisymmetric sudden expansion laminar flow case. Experimental results are used to verify the numerical simulation and GCI outcome. As a result of the application of this method the order of accuracy of the numerical scheme was verified. Additionally, comparing the numerical results with the experimental values, a maximum error of 6% was obtained. Finally, considering the two finest meshes, it can be concluded

that the asymptotic range has been reached and that a finer Mesh won't improve the accuracy of the solution when considering the increased numerical cost.

Keywords: Uncertainty analysis, computational fluid dynamics, Richardson extrapolation, discretization error.

1. INTRODUCCIÓN

The flow studied here consists of laminar flow in a pipe experiencing a sudden expansion. Laminar flow is characterized by low Reynolds number with no lateral mixing. Namely, there are no cross currents perpendicular to the mean direction of flow or eddies. Generally, laminar flow is known by its high momentum diffusion and low momentum convection (Batchelor, 2000; Geankoplis, 2003; Nayak & Bhuvana, 2012). In this particular case the pipe experiences a sudden expansion with a ratio of the outlet diameter to the inlet diameter of 2 (D/d=2, see Fig. 1) resulting in a variety of interesting flow features. At the entrance, the flow has a fully developed velocity profile. At the expansion the flow undergoes separation that in turn produces a recirculation zone. After what is known as the reattachment length, *Lr*, the flow reattaches and there is no more recirculation. The flow achieves a fully developed profile for the new diameter after the redevelopment length, *Ld*.

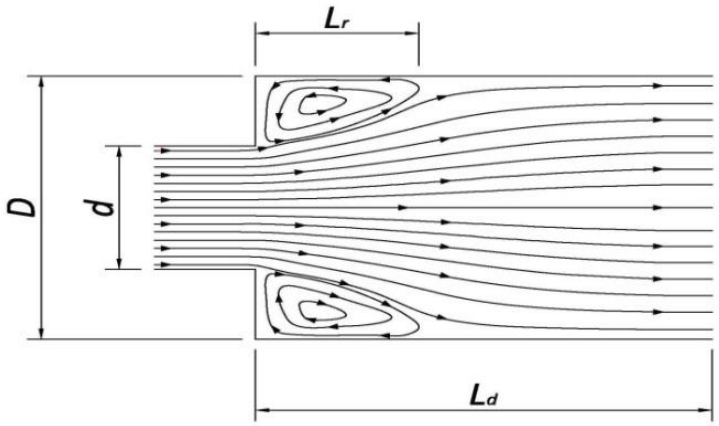

Figure 1. Geometry and flow features for a sudden expansion in a pipe.

The experimental work reported by (Hammad *et al*., 1999) consists of measurements of the velocity field for six different Reynolds numbers, $Re=HU/v$, varying from 20 to 211. H represents the characteristic linear dimension, U the mean velocity and v the kinematic viscosity. The measurements were made with real-time digital particle image velocimetry (PIV). The system is composed of an initial pipe 813 mm long of a diameter of 12.7 mm followed by a sudden expansion (965 mm long) to a 25.4 mm diameter. To avoid flow asymmetry due to buoyancy the experiment fluid is diethylene glycol that has an absolute viscosity of 0.038 Pa at a temperature of 20°C. This value represents 38 times the viscosity of the water allowing the reduction of secondary currents.

The results will be discussed in greater detail later in comparison with the numerical results. However, the main findings of (Hammad *et al*., 1999) are: (1) the velocity field is in fact axisymmetric; (2) the reattachment length shows a minor asymmetry throughout the top and bottom walls of the pipe (nevertheless this irregularity is notably smaller than the uncertainty in the measurements); (3) there is a non-linear relation between the strength of the corner eddies and the Reynolds number; and finally (4) the reattachment and re-development length present an increasing linear profile with increasing Reynolds number. The re-development length was found to be approximately two times the reattachment length.

The numerical simulation was made with OpenFOAM (Open Source Field Operation and Manipulation), an open source computational fluid dynamics (CFD) program. All Reynolds numbers used in the experimental study were simulated. The numerical results were compared with the

experimental findings to determine the level of agreement. Finally the GCI methodology was applied to estimate the uncertainty due to the discretization. It is important to consider that the procedure applied just calculates and reports the error due to the discretization process. There are other sources of error including round-off error and iterative error that are not considered here. The total error estimate is the accumulation of each error.

2. METHODS

2.1. Governing equations and simulation parameters

Considering the domain shown in Fig. 2, the governing equations are the 2D Navier-Stokes equations in cylindrical coordinates (Oosthuizen & Naylor, 1999):

$$\frac{1}{r}\frac{\delta}{\delta r}(vr) + \frac{\delta u}{\delta z} = 0 \tag{1}$$

$$u\frac{\delta u}{\delta z} + v\frac{\delta u}{\delta r} = -\frac{1}{\rho}\frac{\delta p}{\delta z} + v\left(\frac{\delta^2 u}{\delta z^2} + \frac{\delta^2 u}{\delta r^2} + \frac{1}{r}\frac{\delta u}{\delta r}\right) \tag{2}$$

$$u\frac{\delta v}{\delta z} + v\frac{\delta v}{\delta r} = -\frac{1}{\rho}\frac{\delta p}{\delta r} + v\left(\frac{\delta^2 v}{\delta z^2} + \frac{\delta^2 v}{\delta r^2} + \frac{1}{r}\frac{\delta v}{\delta r} - \frac{v}{r^2}\right) \tag{3}$$

where r = distance in radial direction, u = velocity in the radial direction, v = velocity in Z direction, ρ = fluid density, and v = fluid viscosity.

In reality this flow occurs in a 3D space. Nonetheless, it can be modeled in 2D because the flow is axisymmetric (Masatsuka, 2009). The actual flow geometry and the 2D representation are shown in Fig. 2.

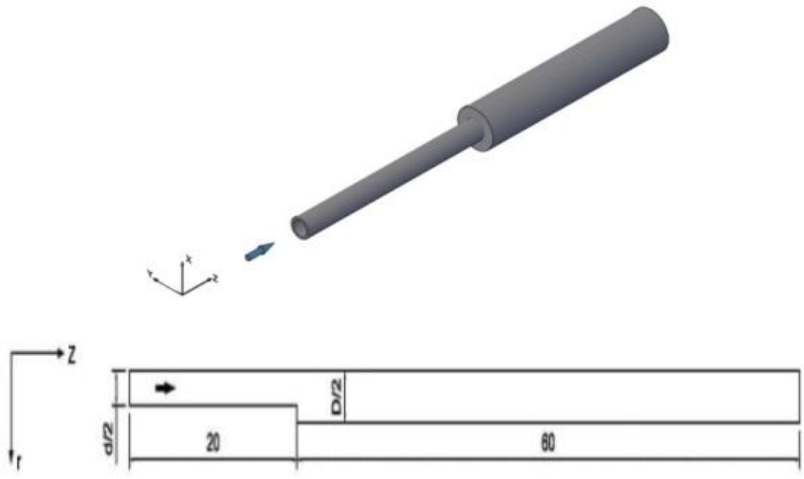

(a)

(b)

Figure 2. (a) Flow domain through a sudden expansion; and (b) Two-dimensional representation of the flow domain. Arrows indicate the direction of flow.

The reduction from 3D to 2D has some benefits, the most important include: (1) a reduction in the computational cost; and (2) a simpler mesh parameters definition. To obtain comparable results Reynolds similarity is applied. To wit, rather than replicate all experimental variables the only parameter that needs to be reproduced exactly is the Reynolds number. The study analyzes six cases with Reynolds numbers of 20.6, 55.4, 77.6, 109, 156.1 and 211.1. For the numerical case, in order to match Reynolds numbers the following conditions were applied. The initial pipe cross-section has a diameter, *d*, of 2 m and the expanded section diameter, *D*, is 4 m to match the expansion ratio of the

laboratory experiments. The inlet pipe has a length of 20 m in the *z* direction and 1 m in the *r* direction. The outlet pipe has a length of 60 m in *z* direction and 2 m in the *r* direction. The kinematic viscosity was adjusted to obtain the desired Reynolds number.

The following boundary conditions were applied to the domain. Along the central axis of the pipe an axisymmetric boundary condition was enforced. The pipe walls were given a wall no-slip, or zero velocity, condition. The entrance of the inlet pipe is given a constant uniform velocity of U=1 m/s for all cases. Additionally at the pipe outlet, a pressure value of zero was assigned.

2.2. Mesh generation

Three grids were used for all Reynolds numbers to analyze the convergence. In all cases the meshes have a uniform size in both the *r* and *z* directions. Starting with the coarse grid, refinement was carried out with a relation fine/coarse grid size of 2. In others words, the mesh density was doubled for each successively finer mesh. A summary of the meshes configuration is presented in Table 1.

Table 1. Mesh configuration.

Mesh	Δz and Δr (m)	Number of cells inlet pipe		Number of cells outlet pipe	
		z direction	*r* direction	*z* direction	*r* direction
Coarse	0.0500	400	20	1200	40
Medium	0.0250	800	40	2400	80
Fine	0.0125	1600	80	4800	160

2.3. Numerical methods and schemes

The numerical method used by OpenFOAM in the present simulation is the finite volume method. The Gauss linear scheme is used for the gradient, divergence, and Laplacian operators. The interpolation scheme is set to linear. Additionally, for the component of gradient normal to a cell face the option orthogonal is selected. The Gauss linear scheme used has second order of accuracy (Open∇Foam, 2014). Simulations were considered converged when the residuals for the continuity, pressure, and momentum equations drop below the value of 1×10^{-6}.

2.4. Richardson extrapolation

Considering the dependent variable *f*, a continuous and differentiable function of a representative grid size, *h*, the error of a numerical solution can be expressed as (Richardson, 1910):

$$E_h = f_{exact} - f_h = C_1 h + C_2 h^2 + C_3 h^3 + \cdots \quad (4)$$

For small values of h and keeping just the leading term the following equations are obtained. f_{exact} is replaced by f_{ext} to denote an extrapolated value:

$$f_{ext} - f_1 = C(\alpha_1 h)^n \quad (5)$$

$$f_{ext} - f_2 = C(\alpha_2 h)^n \quad (6)$$

$$f_{ext} - f_3 = C(\alpha_3 h)^n \quad (7)$$

where C represents a coefficient that can be a function of the coordinates, but not of *h*, *n* the apparent order of the method, and αi and fi (i = 1, 2, 3) are the grid refinement factors (i.e. relation between grid sizes h/h_1, h/h_2, and h/h_3) and the simulated values respectively corresponding to the h_i grid size. h_1 can be assumed equal to *h*. Solving the three previous equations for the three unknowns the following is obtained (Celik & Karatekin, 1997):

$$n = ln[(f_2 - f_3)/(f_1 - f_2)]/ln\,2 \quad (8)$$

$$f_{ext} = (2^n f_1 - f_2)/(2^n - 1) \quad (9)$$

$$C = (f_{ext} - f_1)/h^n \tag{10}$$

2.5. Grid convergence index

The Grid Convergence Index (GCI) methodology emerged as a procedure to determine and report discretization errors estimates in CFD simulations (Roache, 1994). It permits the quantification of the uncertainty present due to grid discretization. This method uses a grid convergence error estimator that is obtained by applying generalized Richardson Extrapolation theory to two different grid size solutions, one on a coarse grid and the other on a fine grid. Through the application of this method an error band for the fine grid solution can be determined. This band is not as an error bound, but a range with a reliable chance of containing the solution (Celik & Zhang, 1995). With the Richardson Extrapolation methodology the following expressions are obtained:

$$GCI\ [fine\ grid] = F_s \frac{|\varepsilon|}{r^p - 1} \tag{11}$$

$$\varepsilon = \frac{f_2 - f_1}{f_1} \tag{12}$$

where F_s = the factor of safety of the method, r = grid refinement ratio (h_2/h_1), and p = the order of accuracy of the numerical solution.

An important consideration requires the determination of the factor of safety, F_s, with recommendations ranging from 1.0 to 3.0 (Celik & Zhang, 1995). A value of 3.0 represents a conservative factor required in cases when a major level of uncertainty of the error estimate exists and when solutions from two grids are used to estimate the error. The necessity of a high factor value increases with the proliferation of uncertainty present in the error estimate. However, a better knowledge or understanding of the processes will allow using smaller values. The general recommendation states a factor F_s = 1.25 when a minimum of three grids are used to verify the order of convergence, p (Roache, 1998).

3. RESULTS

The results corresponding to R_e=20.6 and the medium grid are presented in Fig. 3. First, the whole domain is shown with the corresponding velocity magnitudes (Fig. 3a). It can be verified that after the constant velocity profile assigned at the inlet the profile achieves the fully developed parabolic profile. Subsequently, after the expansion the flow has a decrease in the velocity and a recirculation zone develops. This zone is marked with the smallest velocity values throughout the domain. The recirculation zone can be observed more clearly in Fig. 3b).

In Fig. 4 the centerline velocity, V_c, profile is shown. In the figure the dimensionless parameter V_c/U, is used. For fully developed conditions, the maximum velocity is twice the bulk average velocity (White, 2011). Therefore, from the pipe expansion and normalizing the velocity by the upstream bulk velocity, the centerline velocity profile starts with a value of 2.0 and ends (when the fully developed state is again reached) with a value of 0.5. It can be seen in this figure that the value of 0.5 is attained within the length given in the domain. Specifically this value occurs at z/d=3.28 from the pipe expansion for R_e=20.6. In Fig. 5 the stream lines in the domain are presented. Here both the recirculation zone and the flow redevelopment region can be clearly observed.

The reattachment length was determined by measuring the distance from the expansion to the last point where the flow is negative in the z direction. For each one of the cases the obtained values were compared with the results in (Hammad *et al.*, 1999; Macagno & Hung, 1967).

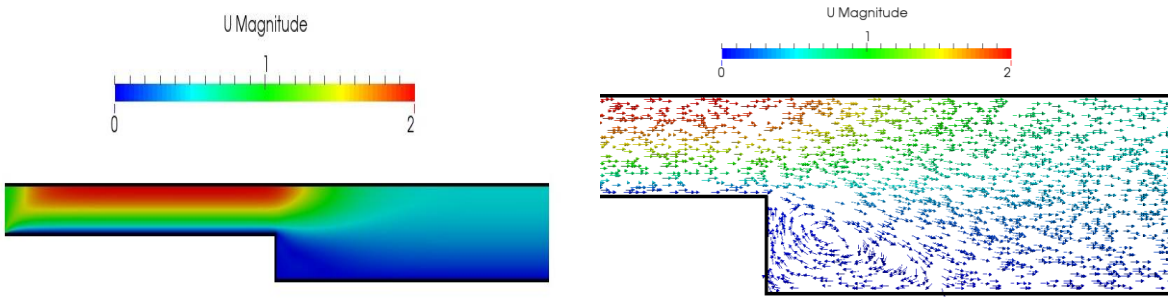

(a) (b)

Figure 3. (a) Contour map of axial velocity magnitude; and (b) Velocity vectors within the recirculation zone.

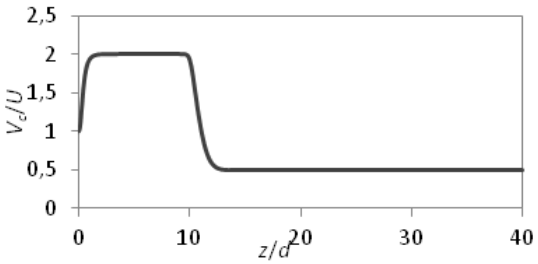

Figure 4. Centerline velocity profile.

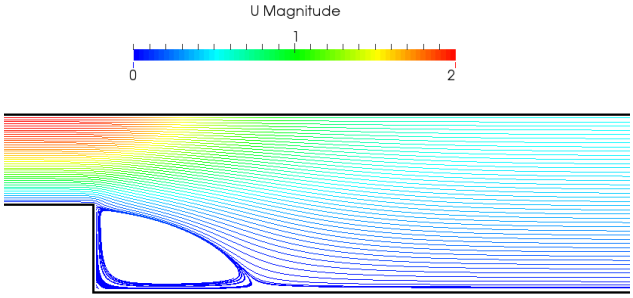

Figure 5. Stream lines in the recirculation zone.

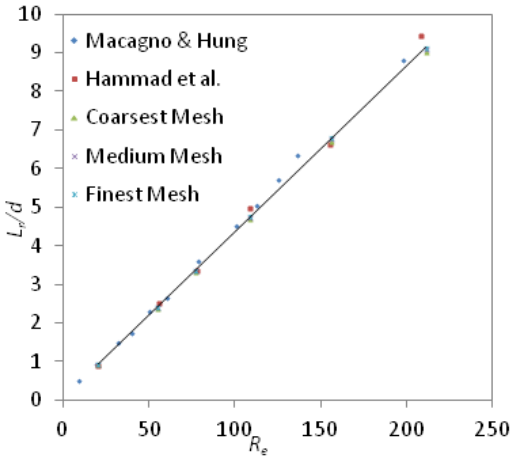

Figure 6. Variation of the reattachment length with Reynolds number. The straight line presented in the graph represents the best fit line for the fine mesh. The other two meshes present a similar profile.

As can be seen in Fig. 6 all the results reported follow a linear tend. The slope reported in (Hammad *et al.*, 1999) is 0.0440. The slopes obtained for each of the grids simulated (fine, medium, and coarse) are 0.0431, 0.0430, and 0.0426 respectively, presenting a percentage difference of 2.0%, 2.3%, and 3.2% from the experimental data. Considering just the result of the numerical simulation, for the three meshes the relation between the reattachment length and the Reynolds number follows a linear profile.

Considering the PIV measurements as a reference, the error in the simulations is presented in Table 2. It can be observed that a tendency related with the Reynolds number is not registered. The error values oscillate with the increase in Reynolds numbers similarly, considering the different grid sizes used the error in some cases increases and in other cases decreases. The greatest error is registered for R_e=109 and the coarse mesh and the smallest for R_e=77.6 and the medium and small meshes.

Table 2. PIV study and numerical simulation results.

R_e	PIV	Coarse mesh		Medium mesh		Fine mesh	
	L_r/d	L_r/d	%	L_r/d	%	L_r/d	%
20.6	0.89	0.92	2.8	0.93	4.3	0.93	4.6
55.4	2.50	2.38	4.8	2.40	3.8	2.41	3.5
77.6	3.37	3.33	1.0	3.37	0.0	3.37	0.0
109	4.98	4.69	5.8	4.74	4.9	4.75	4.7
156.1	6.63	6.71	1.3	6.78	2.2	6.79	2.4
211.1	9.43	9.02	4.4	9.10	3.5	9.11	3.3

3.1. Order of accuracy

The theoretical order of accuracy of the numerical solution is second order. The Richardson Extrapolation method is applied to verify it. Table 3 below shows the results of applying the method.

Table 3. Richardson extrapolation method applied to the simulated reattachment length L_r.

Reynolds Number	f_3 Coarse	f_2 Medium	f_1 Fine	n	f_{ext}
20.6	1.84	1.86	1.87	2.21	1.87
55.4	4.75	4.81	4.82	2.17	4.82
77.6	6.67	6.74	6.76	2.02	6.76
109	9.39	9.48	9.50	2.12	9.50
156.1	13.43	13.55	13.58	2.21	13.58
211.1	18.03	18.19	18.22	2.27	18.23

As can be observed the order of the method is confirmed with all the n values obtained greater than 2. Additionally, in Table 3 the extrapolated value obtained with equation (9) is reported. This value represents a more accurate solution, but as can be seen in the table it does not differ considerably from the fine mesh solution. This value is reported for demonstration purposes, but the further analysis has been conducted with the obtained numerical results.

3.2. Grid convergence index

For the application of this method in the present problem the two finest grids were used. Because the order of accuracy of the method has been confirmed, a factor of safety of 1.25 is used (Roache, 1998; Roache, 2003). Furthermore, the theoretical order (p=2) is maintained for this procedure. The r value is 2 since the grid size is doubled. In Table 4 and Fig. 7 the results of the GCI calculations are presented and compared with the experimental values. As can be seen in the figure, the PIV limits enclose the GCI values (upper, lower and mean). Moreover, the PIV range is much larger than the GCI especially as Reynolds number increases. Furthermore, the GCI limits differ from the numerical solution by less than 0.2%. This leads to the conclusion that the asymptotic range is reached.

Therefore, a finer mesh won't represent a significant improvement to the solution in terms of the discretization error, while the cost of increasing the mesh resolution can grow considerably.

Table 4. GCI and PIV limits of the relation reattachment length/pipe diameter.

Reynolds Number	Numerical solution			GCI Limits		PIV Limits	
	Medium	Fine	GCI	Upper	Lower	Upper	Lower
20.6	0.931	0.934	0.00129	0.935	0.933	1.049	0.629
55.4	2.403	2.409	0.00102	2.410	2.407	2.751	2.105
77.6	3.369	3.378	0.00105	3.379	3.377	3.703	2.917
109	4.738	4.749	0.00092	4.750	4.748	5.482	4.329
156.1	6.775	6.789	0.00081	6.790	6.788	7.310	5.790
211.1	9.096	9.112	0.00075	9.113	9.111	10.461	8.252

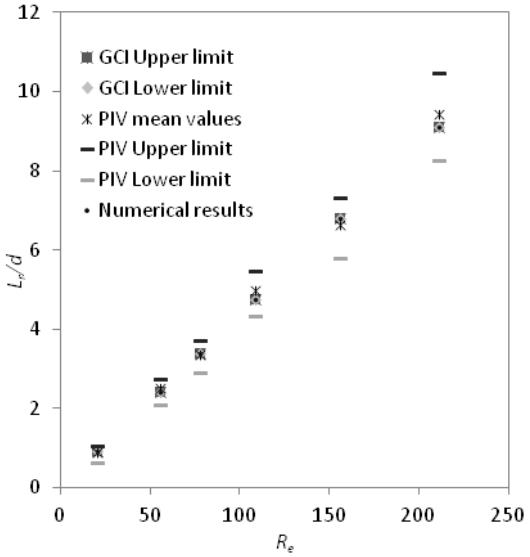

Figure 7. Comparison between GCI and PIV range of variation.

4. CONCLUSIONS

In the present work a numerical analysis of laminar pipe flow with a sudden expansion is presented. The different flow features (recirculation, reattachment, and redevelopment) are observed in the results. For the reattachment length, its behavior was investigated in terms of the numerical solution and also compared with experimental results from the literature. Generally, it can be said that for all cases evaluated (three meshes and six Reynolds numbers) the maximum error due to discretization of the numerical simulation with respect to the experimental results, is around 6%, with a mean error of 3.2%. The relation between the Reynolds number and the reattachment length is confirmed with the numerical results obtaining a linear behavior for the three meshes analyzed with a value of the correlation coefficient (R^2) equal to 1.000 in all cases. There is a maximum 3.2% error in the slope of these lines with respect to the slope reported in the experimental work. Considering the Richardson Extrapolation method and the GCI analysis, the following points are emphasized: (1) the order of convergence of the scheme was verified; (2) the numerical results are within the variation range of the experimental measurements; and (3) the GCI variation is quite small compared with the PIV interval. Therefore, the uncertainty due to discretization has been overcome and the fine mesh can be used with confidence. Additionally, based on the results, it can be said that the grid independence state (asymptotic range) has been reached. Supporting this, in Table 2 can be observed that the medium and fine meshes have almost the same results suggesting that these solutions are in the asymptotic range.

Even though in the present study the discretization error represents a minor percentage of the solution, additional work is needed to determine the other error components and to conclude that the solution is sufficient. Namely, just as with the determination of discretization error, it cannot be verified that the total error is less than the maximum allowed for a numerical solution.

ACKNOWLEDGEMENTS

The first author acknowledges the support of the Fulbright Faculty Development Program.

REFERENCES

Batchelor, G., 2000. *An introduction to fluid dynamics*. New York, Cambridge University Press.

Celik, I., W. Zhang, 1995. Calculation of numerical uncertainty using Richardson extrapolation: Application to some simple turbulent flow calculations. *Journal of Fluid Engineering*, 117, 439-445.

Celik, I., O. Karatekin, 1997. Numerical experiments on application of Richardson extrapolation With nonuniform grids. *ASCE Journal of Fluids Engineering*, 119, 584-590.

Geankoplis, C., 2003. *Transport processes and separation processes principles*. Prentice Hall Professional Technical Reference.

Hammad, K., M.V. Ötügen, E.B. Arik, 1999. A PIV study of the laminar axisymmetric sudden expansion flow. *Experiments in Fluids*, 26, 266-272.

Macagno, E., T.K. Hung, 1967. Computational and experimental study of a captive eddy. » *Journal of Fluid Mechanics*, 28, 43-64.

Masatsuka, K., 2009. *I do like CFD. VOL. 1: Governing equations and exact solutions.*Katate Masatsuka.

Nayak, S., K.P. Bhuvana, 2012. *Engineering Physics*. McGraw-Hill.

Oosthuizen, P.H., D. Naylor, 1999. *An introduction to convective heat transfer analysis.* WCB/McGraw-Hill.

Open∇Foam, 2014. The open source CFD toolbox: User guide. Available at *http://www.openfoam.org/docs/user/index.php*.

Richardson, L., 1910. The approximate arithmetic solution by finite differences of physical problems involving differential equations, with application to stresses in a masonry dam. *Transactions of the Royal Society of London, Series A*, 210, 307-357.

Roache, P., 1994. Perspective: A method for uniform reporting of grid refinement studies. *ASCE Journal of Fluids Engineering*, 116, 405-413.

Roache, P., 1998. *Verification and validation in computational science and engineering.* Hermosa Publishers: Albuquerque.

Roache, P., 2003. Conservatism of the grid convergence index in finite volume computations on steady-state fluid flow and heat transfer. *Journal of Fluids Engineering*, 125, 731-732.

White, F., 2011. *Fluid mechanics.* McGraw-Hill.